A&A manuscript no.
(will be inserted by hand later)

Your thesaurus codes are:
06(03.13.2; 03.13.6; 03.13.5; 06.15.1)

ASTRONOMY AND ASTROPHYSICS

The art of fitting p-mode spectra: Part II. Leakage and noise covariance matrices

Thierry Appourchaux[1], **Maria-Cristina Rabello-Soares**[1], **Laurent Gizon**[1,2]

[1] Space Science Department of ESA, ESTEC, NL-2200 AG Noordwijk
[2] W.W.Hansen Experimental Physics Laboratory, Center for Space Science and Astrophysics, Stanford University, Stanford, CA 94305-4085, USA

Received ; accepted

Abstract. In this article we show how one can apply the theory developed in Part I ('Maximum Likelihood Estimators') to fit real data. We introduce 4 new diagnostics in helioseismology: the (m,ν) echelle diagramme, the cross echelle diagramme, the inter echelle diagramme and the ratio cross spectrum. These diagnostics are extremely powerful to visualize and understand the covariance matrices of the (m,ν) diagrammes, and also to find bugs in the data analysis code. These diagrammes are also used to derive quantitative information on the leakage and noise covariance matrices. Numerous examples using the LOI/SOHO and GONG data are given.

Key words: Methods: data analysis – statistical – observational – Sun: oscillations

1. Introduction

In Appourchaux *et al.* 1997, hereafter Part I, we have described the theoretical background for fitting p-mode Fourier spectra. Using Monte-Carlo simulations, we showed that our fitted parameters were unbiased. We also studied systematic errors due to an imperfect knowledge of the leakage covariance matrix. Unfortunately, a theoretical knowledge of fitting data is not enough as only real data will teach us if our approach is correct. Contrary to fitting p-mode power spectra, the process of fitting the Fourier spectra as described in Part I is rather difficult to understand and visualize. Schou (1992) gave a few diagnostics for understanding how the Fourier spectra are fitted but without showing a way to visualize easily the covariance matrices.

In this paper, we show how one can easily visualize the mode and noise correlation matrices, and then derive the mode leakage matrix. In the first section, we describe 4 new diagrammes that have various diagnostics power. In the second section, we describe how we use those diagrammes for inferring the leakage and noise covariance matrices of the LOI/SOHO data (Appourchaux et al, 1997) and of the GONG data (Hill et al, 1996). The LOI time series starts on 27 March 1996 and ends on 27 March 1997. The GONG time series starts on 27 August 1995 and ends on 22 August 1996. In the last section we conclude by stressing the usefulness of these diagrammes.

Send offprint requests to: T. Appourchaux

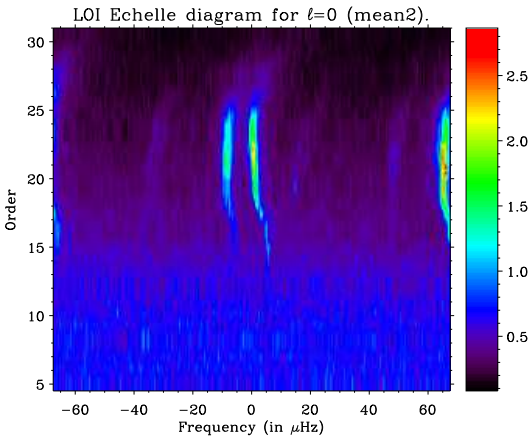

Fig. 1. Power spectra echelle diagramme for 1 year of LOI data seeing the Sun as a star. The $l = 0$ modes are at the center, the $l = 2$ modes are about 10 μHz on the left hand side, the $l = 1$ modes are about +65 μHz on the left hand side, the $l = 3$ can be faintly seen at about 12 μHz from the left hand side of the $l = 1$. Other modes such as $l = 4$ and $l = 5$ can also be seen faintly seen at -35 μHz and +15 μHz, respectively. The distortion of the ridges are due to sound speed gradients in the solar core.

2. Diagnostics for helioseismic data analysis

The echelle diagramme was first introduced by Grec (1981). It is based on the fact that the low-degree modes are essentially equidistant spaced by about 136 μHz. The spectrum is cut into pieces of 136 μHz, and they are stacked on top of each other. Since the modes are not truly equidistant in frequency, the echelle diagramme shows up power

as distorted lines; an example is given in Fig. 1 for the LOI/SOHO instrument seeing the Sun as a star.

Another useful diagramme was introduced by Brown (1985), it is the so-called (m,ν) diagramme which shows how the frequency of an l,m depends upon m. Most often this diagramme is only shown for a single n and for intermediate degrees $l \geq 10$.

The purpose of these diagrammes is always to show an estimate of the variance of the spectra. In our case we also want to visualize not only the variance but also the covariance of the Fourier spectra. Here we briefly recall from Part I that the observed Fourier spectra $(\boldsymbol{y})$ can be related to the individual Fourier spectra of the modes $(\boldsymbol{x})$ by the leakage matrix $\mathsf{C}^{(l,l')}$ by:

$$\boldsymbol{y} = \mathsf{C}^{(l,l')}\boldsymbol{x} \tag{1}$$

The covariance matrix of $\mathrm{Re}(\boldsymbol{y})$, or of $\mathrm{Im}(\boldsymbol{y})$, can be derived from the sub-matrix $\mathcal{V}^{(l,l')}$ of the covariance matrix $\mathsf{V}^{(l,l')}$. The real part of the elements of the sub-matrix can be expressed as:

$$2\mathcal{V}^{(l,l')}_{m,m'} = E[y_{l,m}(\nu)y^*_{l',m'}(\nu)] =$$
$$2\sum_{l"=l,l'}\sum_{m"=-l"}^{m"=l"} \mathsf{C}^{(l',l")}_{m',m"}\mathsf{C}^{(l,l")}_{m,m"} f^{l"}_{m"}\nu + 2\mathsf{B}^{(l,l')}_{m,m'} \tag{2}$$

where $f^{l"}_{m"}(\nu)$ is the profile of the $l"$, $m"$ mode and $\mathsf{B}^{(l,l')}$ is the covariance matrix of the noise. Equation 2 contains all the information that we need for visualizing an estimate of the real and imaginary parts of $\mathcal{V}^{(l,l')}$. Drawing from the usefulness of the diagrammes of Grec and Brown, we created four new diagrammes for visualizing an estimate of the real part of $\mathcal{V}^r$, all having various diagnostics power:

1. (m,ν) echelle diagramme: estimate of the diagonal elements of $\mathcal{V}^{(l,l)}$ (same l)
2. cross echelle diagramme: estimate of the off-diagonal elements of $\mathcal{V}^{(l,l)}$ (same l)
3. inter echelle diagramme: estimate of the off-diagonal elements of $\mathcal{V}^{(l,l')}$ (different l)
4. ratio cross spectrum: estimate of the ratio of the elements of $\mathsf{B}^{(l,l')}$

Each diagnostic is described hereafter in more details.

2.1. (m,ν) echelle diagramme

The (m,ν) *echelle diagramme* is made of $2l+1$ echelle diagrammes of each l,m power spectra or $|y_{l,m}(\nu)|^2$. The $2l+1$ echelle diagrammes are stacked on top of each other to show the dependence upon m of the mode frequency. These diagrammes give an estimate of the diagonal of the covariance matrix of the observations as:

$$2\widetilde{\mathcal{V}}^{(l,l')}_{m,m'}(\nu) = |y_{l,m}(\nu)|^2 \tag{3}$$

where $\widetilde{\mathcal{V}}$ symbolize the estimate. The factor 2 comes from the fact that $\mathcal{V}$ represents both the covariance of the real parts of the Fourier spectra, and of the imaginary parts (See Part I, section 3.3.2).

Example of diagrammes can be seen in Fig. 2. It is important when one makes those diagrammes to tune the spacing for the degree to study. For example, one can see in Fig. 2 that the ridges of power of $l = 0, 1, 2$ and 3 have different shapes. Other modes with a significant different spacing can be seen more like diagonal lines crossing the (m,ν) diagrammes; this is a powerful tool to identify other degrees.

When the leakage matrix is real, as it is most often the case, the theoretical covariance matrix of the Fourier spectra, for $l = 1$ for example, can be written as:

$$\mathcal{V}^{(1,1)}(\nu) = \begin{pmatrix} f^1_1\nu + \alpha^2 f^1_{-1}\nu & 0 & \alpha(f^1_1\nu + f^1_{-1}\nu) \\ 0 & f^1_0\nu & 0 \\ \alpha(f^1_1\nu + f^1_{-1}\nu) & 0 & f^1_{-1}\nu + \alpha^2 f^1_1\nu \end{pmatrix} + \begin{pmatrix} b_1 & 0 & \beta b_1 \\ 0 & b_0 & 0 \\ \beta b_1 & 0 & b_1 \end{pmatrix} \tag{4}$$

where the $f^l_m\nu$ is the variance of the m-th mode, α is the off-diagonal elements of the leakage matrix which is given by:

$$\mathsf{C}^{(1,1)} = \begin{pmatrix} 1 & 0 & \alpha \\ 0 & 1 & 0 \\ \alpha & 0 & 1 \end{pmatrix}$$

Unfortunately the diagnostics power of the (m,ν) echelle diagrammes is rather limited for deriving the leakage matrix. First, the sign information on α disappears; second, the magnitude of α being typically less than 0.5, the leakage cannot be easily seen in the power spectra. Another kind of diagramme more useful had to be devised.

2.2. Cross echelle diagramme

The *cross echelle diagramme* is made of $2l+1$ echelle diagrammes of each real part of the cross spectrum of m and m' or $y_{l,m}(\nu)y^*_{l,m'}(\nu)$. The $2l+1$ real parts of the cross spectra are stacked on top of each other to show the dependence upon m of the mode frequency. These diagrammes give an estimate of the rows (or columns) of the covariance matrix of the observations as:

$$2\widetilde{\mathcal{V}}^{(l,l')}_{m,m'}(\nu) = y_{l,m}(\nu)y^*_{l,m'}(\nu) \tag{5}$$

The factor 2 is here for the same reason as for the (m,ν) echelle diagramme. Of course when $m = m'$ we get the echelle diagrammes of the previous section. An example of a diagramme can be seen in Fig. 3. Only $l+1$ cross echelle diagrammes are shown as the covariance matrices are symmetrical.

The imaginary part of the cross spectra has some diagnostic power: it represents correlation between the real and imaginary parts of the Fourier spectra. When the leakage matrix is real, there is no correlation between the real and imaginary parts; nevertheless this could be helpful to

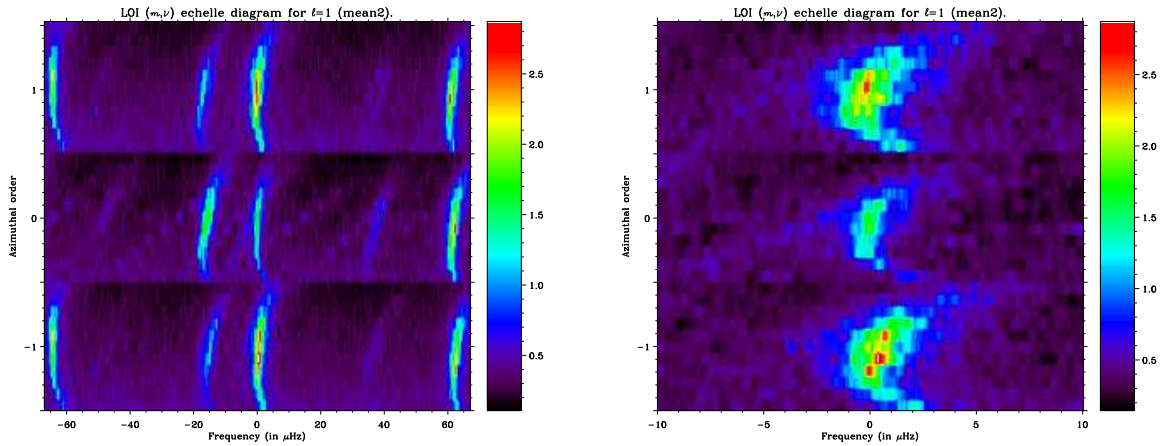

Fig. 2. (m, ν) echelle diagramme of 1 year of LOI data for $l = 1$. (Left) The full diagramme centered on $l = 1$ with a spacing of 134.8 μHz. The $l = 3$ modes are located about 11 μHz at the left of the $l = 1$. The $l = 2$ modes are on the right edge, while the $l = 0$ are on the opposite side. Other indications $l = 4$ modes can be seen around +40 μHz. (Right) The same diagramme but enlarged around $l = 1$. The frequency shift or splitting of the modes due to the solar rotation is clearly visible. The artificial correlation between $m = -1$ and $m = +1$ is not as clear.

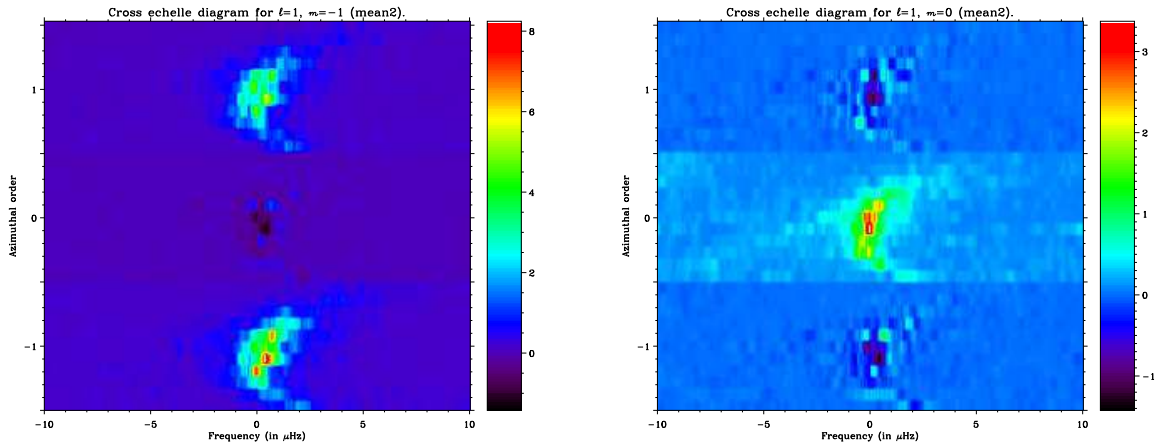

Fig. 3. Cross echelle diagrammes of 1 year of LOI data for $l = 1$. (Left) For $l = 1, m = -1$. The lower panel represents the echelle diagramme of $m = -1$. The 2 other panels are the cross spectra with $m = 0$ and $m = 1$. There is no visible correlation between $m = -1$ and $m = 0$ while there is between $m = -1$ and $m = +1$. Here we visualize the first line of Eq. 4. (Right) For $l = 1, m = 0$. The bottom panel is the same as the middle panel of the left diagramme but with a different color scale. The middle panel is the power spectra of $m = 0$ already shown in Fig. 2; the $l = 6$ is more visible, thanks to a different color scale.

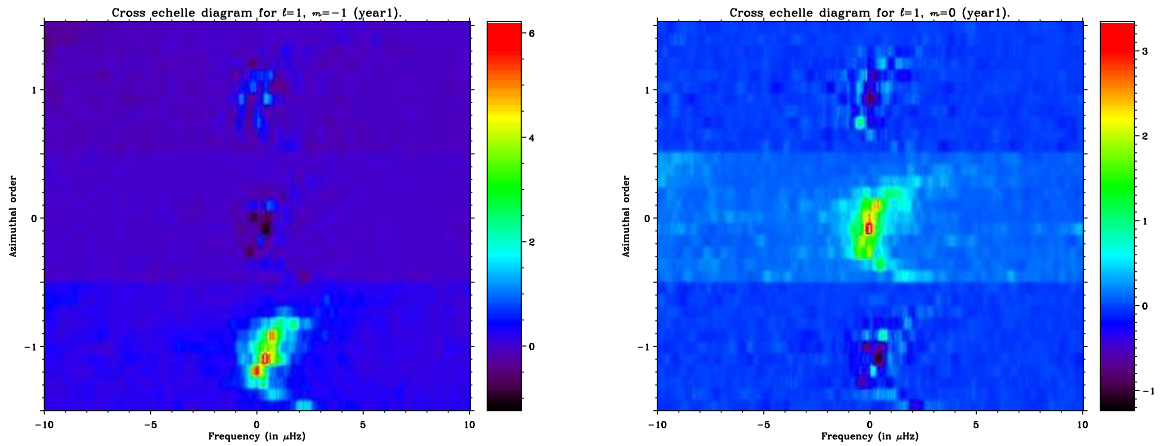

Fig. 4. Cross echelle diagrammes of 1 year of LOI data for $l = 1$. The inverse of the theoretical leakage matrix has been applied to the original data with α=0.474. (Left) For $l = 1, m = -1$. The artificial correlation between $m = -1$ and $m = +1$ has been entirely removed. (Right) For $l = 1, m = 0$. There is no improvement as there were no correlation before.

find errors in the filters applied to the images (See Part I, section ? and later in this article).

As we can see with Eq. 4, these diagrammes preserve the sign of α. For $l = 1$, it is quite straightforward to derive the sign of α. We show hereafter that the sign of other elements of the leakage matrix can be derived but with more thinking. It can be shown that the elements of $\mathcal{V}$ can be expressed as:

$$\mathcal{V}^{(l,l)}_{m,m'} = \mathsf{C}^{(l,l)}_{m,m'} f^l_{m'}\nu + \mathsf{C}^{(l,l)*}_{m',m} f^l_m \nu + \sum_{m" \neq m',m} \mathsf{C}^{(l,l)}_{m',m"} \mathsf{C}^{(l,l)*}_{m,m"} f^{l"}_{m'}(\nu) + \mathsf{B}^{(l,l)}_{m,m'} \quad (6)$$

In general, the cross spectra for m, m', representing $\mathcal{V}^{(l,l)}_{m,m'}$ carries information over the sign of the leakage elements $\mathsf{C}^{(l,l)}_{m,m'}$ and $\mathsf{C}^{(l,l)*}_{m',m}$. This is a very general property for any cross echelle diagramme of a given degree. The other additional terms expressed as product of leakage elements are sometimes more difficult to interpret: they carry some information about other leakage elements.

But the power of these diagrammes is not only limited to checking the sign of the elements of the leakage matrix. They are real tools to get a first order estimate of the leakage matrix. We have shown in Part I, that there is no difference between fitting data for which the leakage matrix is *not* diagonal, and data for which the leakage *is* diagonal. We showed in part I, that the covariance matrix of $\boldsymbol{x} = \mathsf{C}^{-1}\boldsymbol{y}$ can be written (similarly to Eq. 2) by the sum of 2 matrices: the first one represents the mode covariance matrix and is diagonal, and the second term represents the covariance matrix of the noise. Therefore, applying the inverse of the leakage matrix to the data should, in principle, remove all artificial mode correlations between the Fourier spectra: Fig. 4 shows the result of this cleaning for $l = 1$. To the first order, there is no mode correlation left. This is the most powerful test for deriving the leakage matrices.

The cross echelle diagrammes are useful to verify the correlation within a given degree, but other degrees leak into the target degree, such as $l = 6$, 7 and 8 into $l = 1$, 4 and 8, respectively. The purpose of the next diagramme is to assess the magnitude of this leakage.

2.3. Inter echelle diagramme

The *inter echelle diagramme* of an l, m mode for the degree l' is made of $2l' + 1$ echelle diagrammes for each real part of the cross spectrum of l, m and l', m' or $y_{l,m}(\nu)y^*_{l',m'}(\nu)$. The $2l' + 1$ real part of the cross spectra are stacked on top of each other to show the dependence upon m'. These diagrammes give an estimate of the rows (or columns) of the covariance matrix of the observations as:

$$2\widetilde{\mathcal{V}}_{m,m'}(\nu) = \mathrm{Re}(y_{l,m}(\nu)y^*_{l',m'}(\nu)) \quad (7)$$

Similarly as for the cross echelle diagramme, it will help to visualize the covariance matrix between different degrees, and to derive leakage elements of the full leakage matrix $\mathsf{C}^{l'}_l$. One can derive an equation resembling Eq. 6 for different degrees that can show the inter echelle diagramme carries information over the sign of the leakage elements $\mathsf{C}^{(l,l')}_{m,m'}$ and $\mathsf{C}^{(l',l)*}_{m',m}$.

Figures 5 shows this diagramme for $l = 1$ and $l' = 6$. These diagrammes are more difficult to interpret, but using specific spacing for l or l', one can identify without ambiguity which degree contribute to the correlation. As mentioned above applying the inverse of the leakage matrix will help to verify to the first order that there is no correlation. When different degrees are involved the full leakage matrix $\mathsf{C}_{(l,l')}$ has to be used, and it will lead to similar cleaned diagrammes as Fig. 4.

2.4. Ratio cross spectrum

All the previous diagrammes are helpful to understand and visualize the mode covariance matrices. Unfortunately, these diagrammes are useless to evaluate the correlation of the noise in the Fourier spectra. In between the p modes, these correlations can be more easily visualized as we have:

$$\mathcal{V}^{(l,l)}_{m,m'} \approx \mathsf{B}^{(l,l)}_{m,m'} \quad (8)$$

But instead of visualizing $\mathsf{B}^{(l,l')}$, we prefer to look directly at the correlation by computing the ratio of the cross spectra as:

$$\frac{\widetilde{B^{(l,l')}_{m,m'}}}{B^{(l,l)}_{m,m}} = \frac{\mathrm{Re}(y_{l,m}(\nu)y^*_{l,m'}(\nu))}{|y_{l,m}(\nu)|^2} \quad (9)$$

The real part of this ratio is called the *ratio cross spectrum*. The ratio cross spectrum is a very direct way to derive the noise covariance matrix which is needed by the fitting routines. For example from Eq. 4, it can be derived that this is a good way to visualize β. The ratio gives a better understanding of how much the noise background is correlated between the Fourier spectra.

Figure 6 show the ratio cross spectra for $l = 1$. In the p-mode frequency range, this ratio is more difficult to interpret as the noise correlation is affected by the presence of the modes. Nevertheless by looking away from the modes (at high or low frequency) or by looking between the modes, one could get a reasonable good estimate of the noise covariance. The leakage and noise covariance matrices have similar properties. For example, there is no correlation between the m for which $m + m'$ is odd for either matrix. This lack of correlation can be seen in Fig. 6. The ratio is also useful if one wants to reduce the number of noise parameter to be fitted. This is useful when the noise background, mainly of solar origin, varies slowly over the p-mode range; then the ratio can be assumed to be constant over the p-mode range. For example for $l = 1$ we can fit 2 noise parameters instead of 3. When the noise varies in the p-mode range, it is more advisable to fit as much noise parameters as needed.

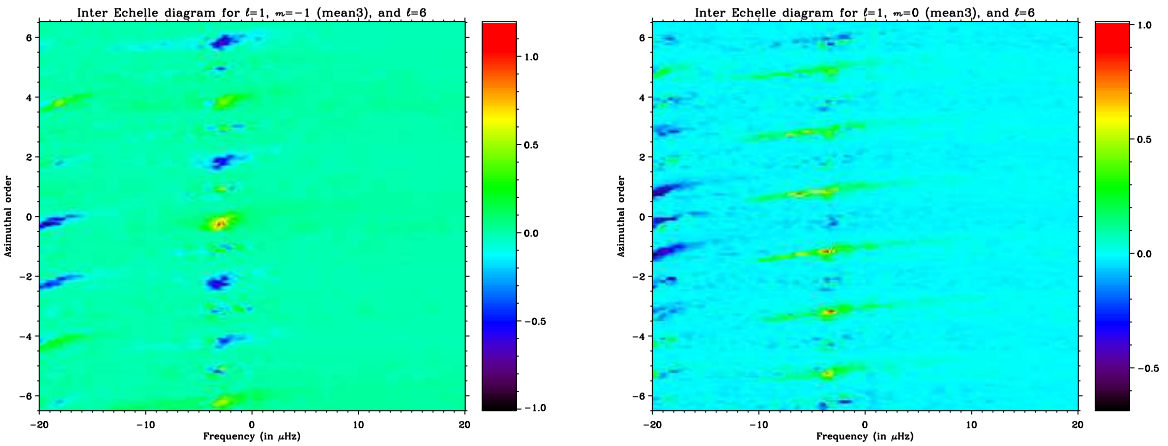

Fig. 5. Inter echelle diagrammes of 1 year of LOI data for $l = 1$ and $l' = 6$. (Left) For $l = 1, m = -1$. Given the structure of the ridges, it means that the $l = 1$ modes leak into the even m modes of $l' = 6$, while the $l' = 6$ modes do not leak into the $l = 1$. (Right) For $l = 1, m = 0$. Again using the structure of the ridges, the odd m' of $l' = 6$ leaks weakly into $l = 1, m = 0$.

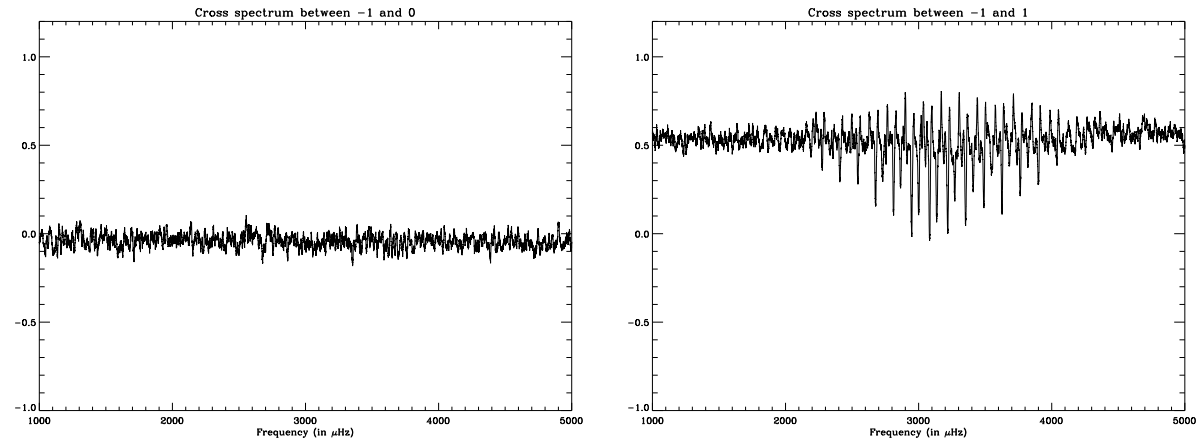

Fig. 6. Ratio cross spectra for $l = 1$. (Left) For $m = -1$ and m'=0. There is very little correlation, less than -0.05. The modes also are not seen. (Right) For $m = -1$ and $m = 1$. The noise correlation is about 0.55. The modes are visible with various positive and negative correlation.

3. Application to data

3.1. A useful detail

Before using these diagrammes on real data, we need to point out a very important property coming from the way the m signals are built. If the weights applied to the images have the same properties as of the spherical harmonics then we have:

$$W_{l,m} = W^*_{l,-m} \tag{10}$$

which means that both the signal of $+m$ and $-m$ can be obtained from using a single filter $W_{l,m}$. The signal of $+m$ will be in the positive part of the frequency range, while the *conjugate* of the signal of $-m$ will be in the negative range. This latter fact is very important, if one does not take care of the sign of the imaginary part of $-m$, it will lead to very serious problem. Needless to say that fitting data without taking into account this detail will have devastating effects. Figure 7 shows cross echelle diagrammes for the real and imaginary parts of the spectra of $l = 2$; the latter part had no sign compensation for $m < 0$. Obviously this important detail cannot be detected in the power spectra.

3.2. Leakage matrix measurement

3.2.1. LOI/SOHO data

Figure 2,8 and 9 show the (m, ν) echelle diagramme for 1 year of LOI data for $l = 1, 2$ and 5, respectively. In each of those diagrammes, various spurious degrees are detected. The $l = 5$ (m, ν) echelle diagramme is clearly polluted by an other degree: $l = 8$. It appears in a different way depending on m. For $l = 5, m = -5$, the $l = 8, m = +8$ is quite strong; while for $l = 5, m = +5$, this is $l = 8, m = -8$ which shows up. This kind of 'anti'-splitting behaviour is typical of any aliasing degrees. It is more prominent in the

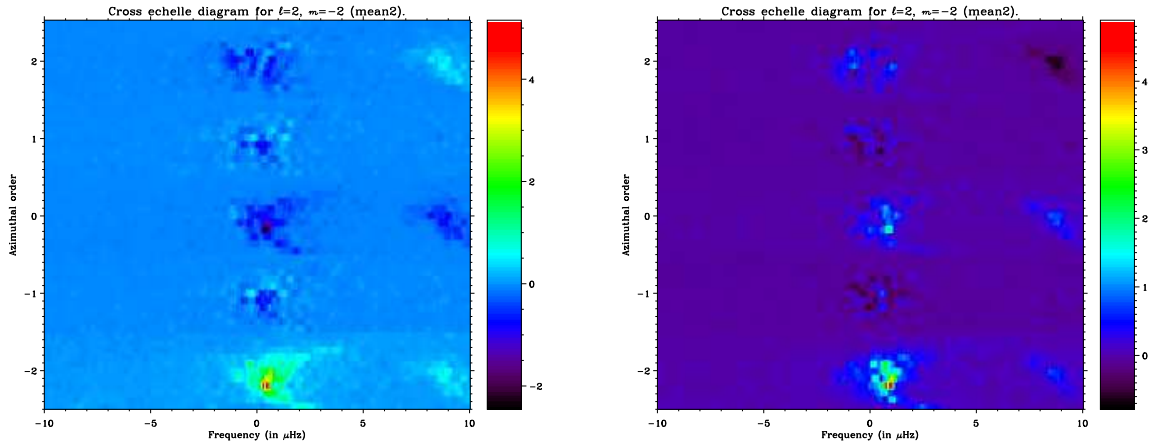

Fig. 7. Effect of a wrong sign on the cross echelle diagrammes of 1 year of LOI data for $l = 2, m = -2$. (Left) For the real parts or $\mathrm{Re}(y_{l,m}(\nu))\mathrm{Re}(y_{l,m'}(\nu))$. (Right) For the imaginary parts or $\mathrm{Im}(y_{l,m}(\nu))\mathrm{Im}(y_{l,m'}(\nu))$ without having the sign corrected. The cross echelle diagramme is built by the sum of those 2 quantities; compensation due to different signs will be misleading. The correlation of the real parts will always have the correct sign; this can be used for checking the correlation of the imaginary parts.

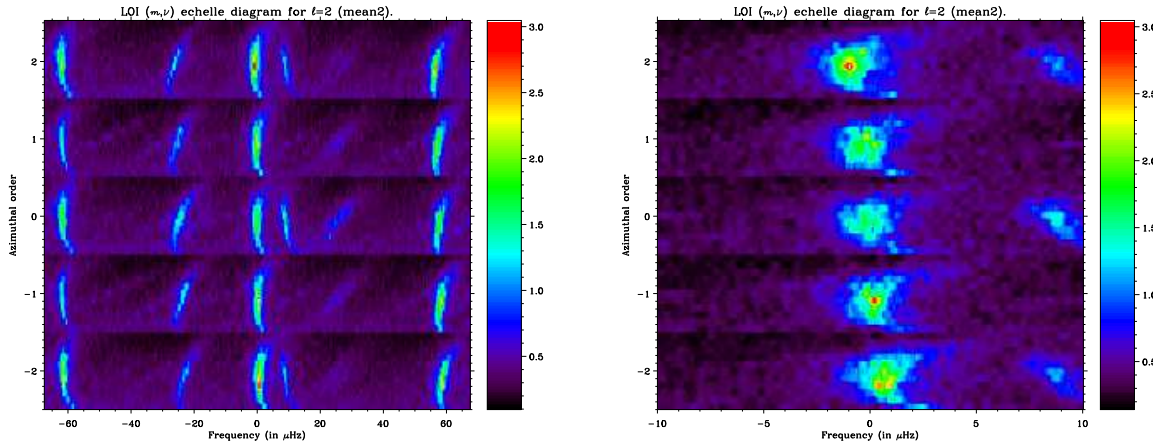

Fig. 8. (m, ν) echelle diagramme of 1 year of LOI data for $l = 2$. (Left) The full diagramme centered on $l = 2$ with a spacing of 135. μHz. The $l = 0$ modes are located about 10 μHz at the right of the $l = 0$. The $l = 3$ modes are on the right edge, while the $l = 1$ are on the opposite side. The $l = 4$ modes is easily seen at about -25 μHz; the $l = 5$ starts to appear at +25 μHz. (Right) The same diagramme but enlarged around $l = 2$ with the $l = 0$ at the right hand side. The splitting of the modes is clear. Please note the absence of the $l = 0$ mode for $m = \pm 1$

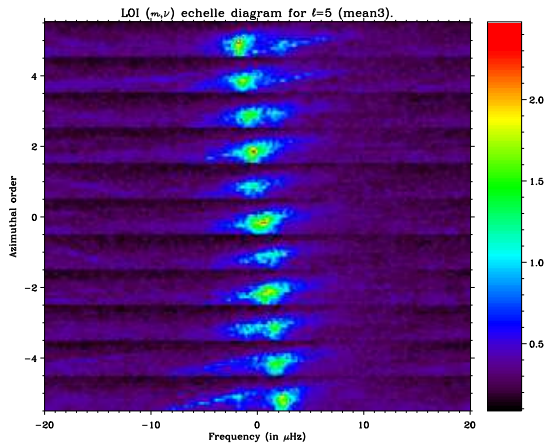

Fig. 9. (m, ν) echelle diagramme of 1 year of LOI data for $l = 5$ with a spacing of 136 μHz. Here we can clearly see the splitting of the $l = 5$ modes. Unfortunately, the $l = 5$ data of the LOI are heavily polluted by the presence of the $l = 8$. But since the spacing for the $l = 8$ is different that of the $l = 5$, the $l = 8$ are seen lines of power going from lower left to upper right at each m while the $l = 5$ are seen more like straight ridges. It can also be seen that the $|m| = 5$ Fourier spectra contain information both about $m = \pm 5$. This is the result of the large LOI pixel size creating oversampling. The $l = 8$ are also differentiated because the 'splitting' of this alias is in the opposite direction that of the $l = 5$.

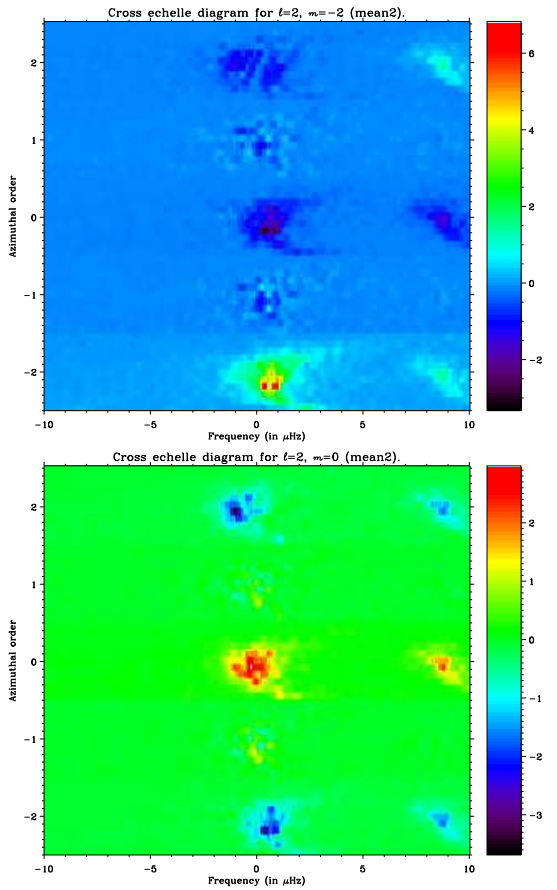

Fig. 10. Cross echelle diagrammes of 1 year of LOI data for $l = 2$. (Top, left) For $m = -2$. The middle panel (for $m' = 0$), representing $M_{-2,0} = M_{0,-2}$, has negative 'power' close to the frequencies of the $m = -2$, indicating that α_3 is negative. There is some indication that α_1 may be negative. The upper panel (for $m' = 2$), , representing $M_{-2,2} = M_{2,-2}$, has 2 patches of negative 'power' close to the frequencies of $m = -2$ and $m = +2$, showing that α_4 is also negative. (Top, right) For $m = -1$. Here it is obvious that α_2 is positive. (Opposite) For $m = 0$. There is now 2 patches of negative power in 2 opposite panels ($m' = -2$ and $m' = 2$) due to the negativity of α_3. It is likely that α_1 is also negative.

LOI data because of the undersampling effect due to the large size of the LOI pixels.

Figure 3, 10 and 12 display the cross echelle diagramme for $l = 1, 2$ and 5, respectively. We have already shown that our knowledge of the leakage matrix of $l = 1$ was quite good. For other degrees, the situation gets more complicated with even more leakage matrix elements to evaluate. Hereafter we give the mode covariance for $l = 2$, where we can see that the sign derivation of the leakage matrix elements is less obvious. For $l = 2$, the leakage matrix can be written as:

$$C^{(2,2)} = \begin{pmatrix} 1 & 0 & \alpha_1 & 0 & \alpha_4 \\ 0 & 1 & 0 & \alpha_2 & 0 \\ \alpha_3 & 0 & 1 & 0 & \alpha_3 \\ 0 & \alpha_2 & 0 & 1 & 0 \\ \alpha_4 & 0 & \alpha_1 & 0 & 1 \end{pmatrix} \quad (11)$$

Using Eq. 6, we can derive that the cross echelle diagramme between $m = -1$ and $m = +1$ will give the sign of α_2, between $m = -2$ and $m = +2$ of α_4, between $m = \pm 2$ and $m = 0$ of α_3 and α_1. As shown by Fig. 10, the sign of the leakage matrix elements could be derived without difficulties.

According to theoretical computation of the p-mode sensitivities of the LOI pixels (Appourchaux and Andersen, 1990) and using the real shape of the LOI pixels (Appourchaux and Telljohann, 1996), the leakage matrices of $l = 2$ is given by:

$$C^{(2,2)} = \begin{pmatrix} 1 & 0 & -0.308 & 0 & -0.216 \\ 0 & 1 & 0 & 0.576 & 0 \\ -0.308 & 0 & 1 & 0 & -0.308 \\ 0 & 0.576 & 0 & 1 & 0 \\ -0.216 & 0 & -0.308 & 0 & 1 \end{pmatrix}$$

The leakage matrix of $l = 5$ is given in Table .1. These leakage matrices are mean value over one year. The leakages vary throughout the year because the distance between the SOHO spacecraft (or the Earth) varies. There is no B angle effect as the mean B is zero over 1 year. We have already shown that our knowledge of the leakage matrix of $l = 1$ was quite good (See Fig.4). From the cross echelle diagramme, we can directly verify that the sign, and sometimes even the magnitude of the leakage elements (See Fig. 10).

The best cross check that our theoretical computations are correct is to apply the inverse of the leakage matrices to the original data. Figure .11 shows how the artificial correlations can be removed from the LOI data; here we also cleaned the original data from the presence of the $l = 0$ modes. Unfortunately, the leakage matrix of $l = 5$ for the LOI data cannot be inverted. This is the result of the pixel undersampling. This results has a two dramatic consequence: the leakage matrix cannot be verified as for

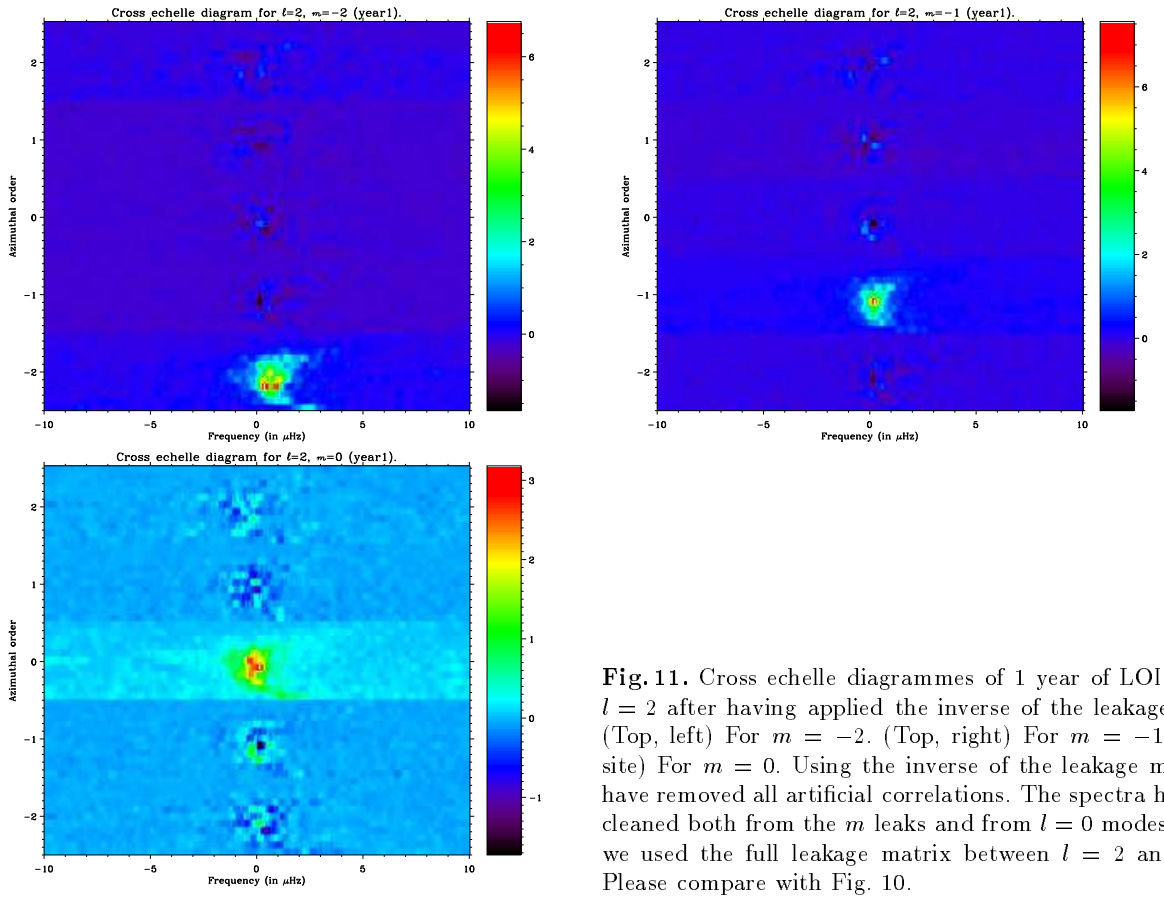

Fig. 11. Cross echelle diagrammes of 1 year of LOI data for $l = 2$ after having applied the inverse of the leakage matrix. (Top, left) For $m = -2$. (Top, right) For $m = -1$. (Opposite) For $m = 0$. Using the inverse of the leakage matrix we have removed all artificial correlations. The spectra have been cleaned both from the m leaks and from $l = 0$ modes because we used the full leakage matrix between $l = 2$ and $l = 0$. Please compare with Fig. 10.

Table 1. Theoretical leakage matrix of l=5 for the LOI data.

		m'										
		-5	-4	-3	-2	-1	0	1	2	3	4	5
	-5	1	0	0.18	0	-0.10	0	0.08	0	0.19	0	-0.45
	-4	0	1	0	0.27	0	-0.13	0	0.17	0	0.03	0
	-3	0.18	0	1	0	0.64	0	-0.21	0	-0.62	0	0.19
	-2	0	0.27	0	1	0	0.50	0	-0.18	0	0.17	0
	-1	-0.10	0	0.64	0	1	0	0.52	0	-0.21	0	0.08
m	0	0	-0.13	0	0.50	0	1	0	0.50	0	-0.13	0
	1	0.08	0	-0.21	0	0.52	0	1	0	0.64	0	-0.10
	2	0	0.17	0	-0.18	0	0.50	0	1	0	0.27	0
	3	0.19	0	-0.62	0	-0.21	0	0.64	0	1	0	0.18
	4	0	0.03	0	0.17	0	-0.13	0	0.27	0	1	0
	5	-0.45	0	0.19	0	0.08	0	-0.10	0	0.18	0	1

the $l = 2$, and fitting the data as described in Part I is not valid anymore as the leakage matrix needs to be invertible. It means that the $2l+1$ Fourier spectra of $l = 5$ are dependent. A way around it would be to restrict the fitting to truly independent Fourier spectra. This problem is specific to the LOI data and applies only for $l \geq 4$.

As shown by Fig. 12 and 9 other degrees can be detected in the targeted degrees. For the LOI data, the $l = 5$ and $l = 8$ (similarly $l = 4$ and $l = 7$) are more affected by each other than for the GONG data. This is due again to the spatial undersampling. Fortunately, the $l = 1$ LOI data are far less affected by the presence of $l = 6$ that of GONG (See in the next section); this is the result of an effective apodization function (limb darkening) which creates a narrower spatial response than that of GONG (line-of-sight projection). We will see later on with the GONG data that cleaning, similar as for the $l = 0$ and $l = 2$ of the LOI, can be achieved not only for 2 degrees but also for 3 degrees ($l = 1, 6$ and 9).

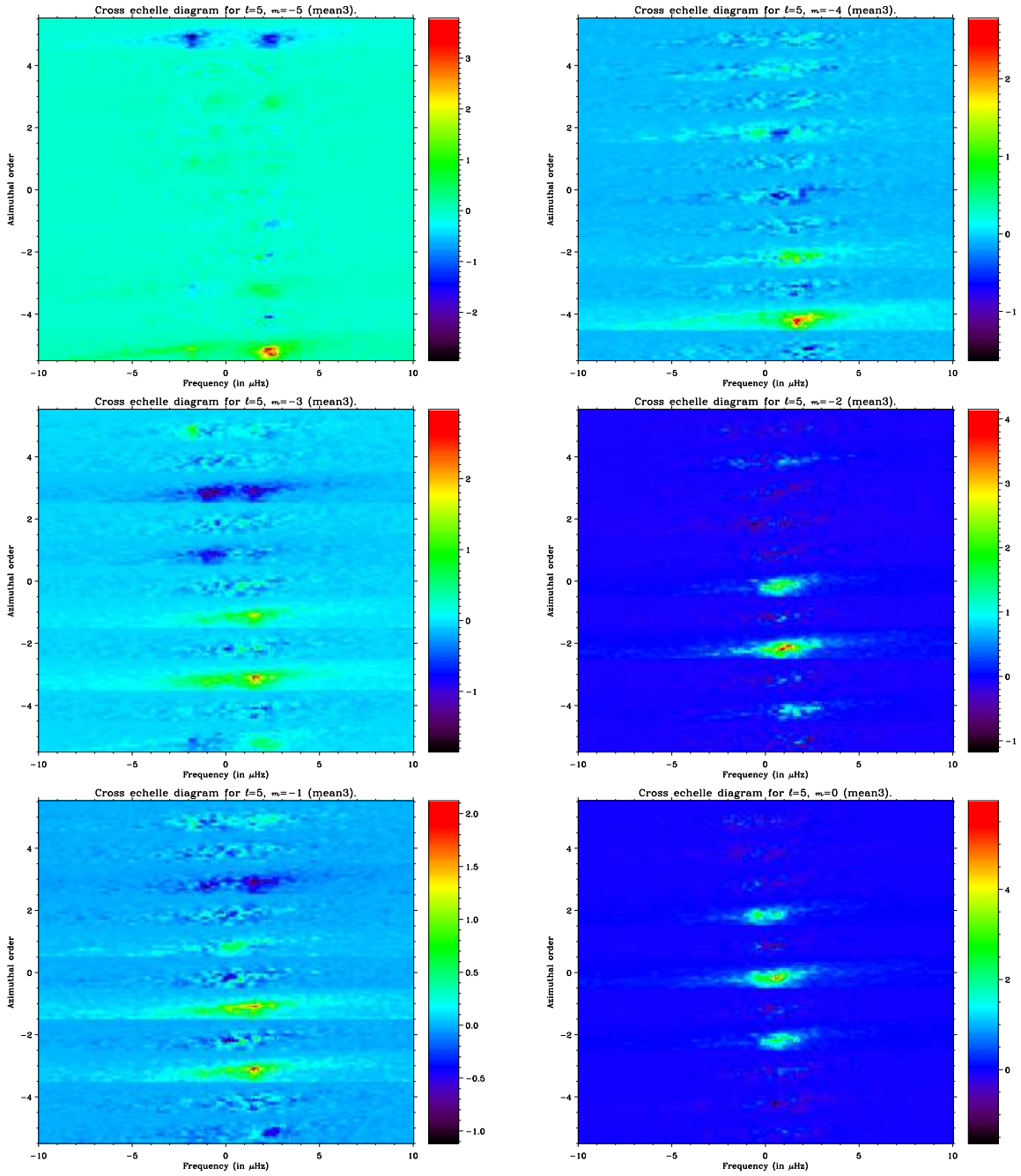

Fig. 12. Cross echelle diagrammes of 1 year of LOI data for $l = 5$. (Top, left) For $m = -5$. Here we can see the strong leakage of $m' = 5$ into $m = 5$ and vice versa. The 2 patches of negative 'power' on the upper panel (or positive on the lower panel) are the $m = \pm 5$ modes separated by about 4-5 μHz. (Top, right) For $m = -4$. Leakages between $m = -4$ and $m = -2$ are visible, but weaker than for $m = -5$. (Middle, left) For $m = -3$. Strong leakages between $m = -3$ and $m = +3$. (Middle, right) For $m = -2$. (Bottom, left) For $m = -1$. (Bottom, right) For $m = 0$. The left diagrammes show more leakages that of the right ones, the $l + m$ parity makes the difference.

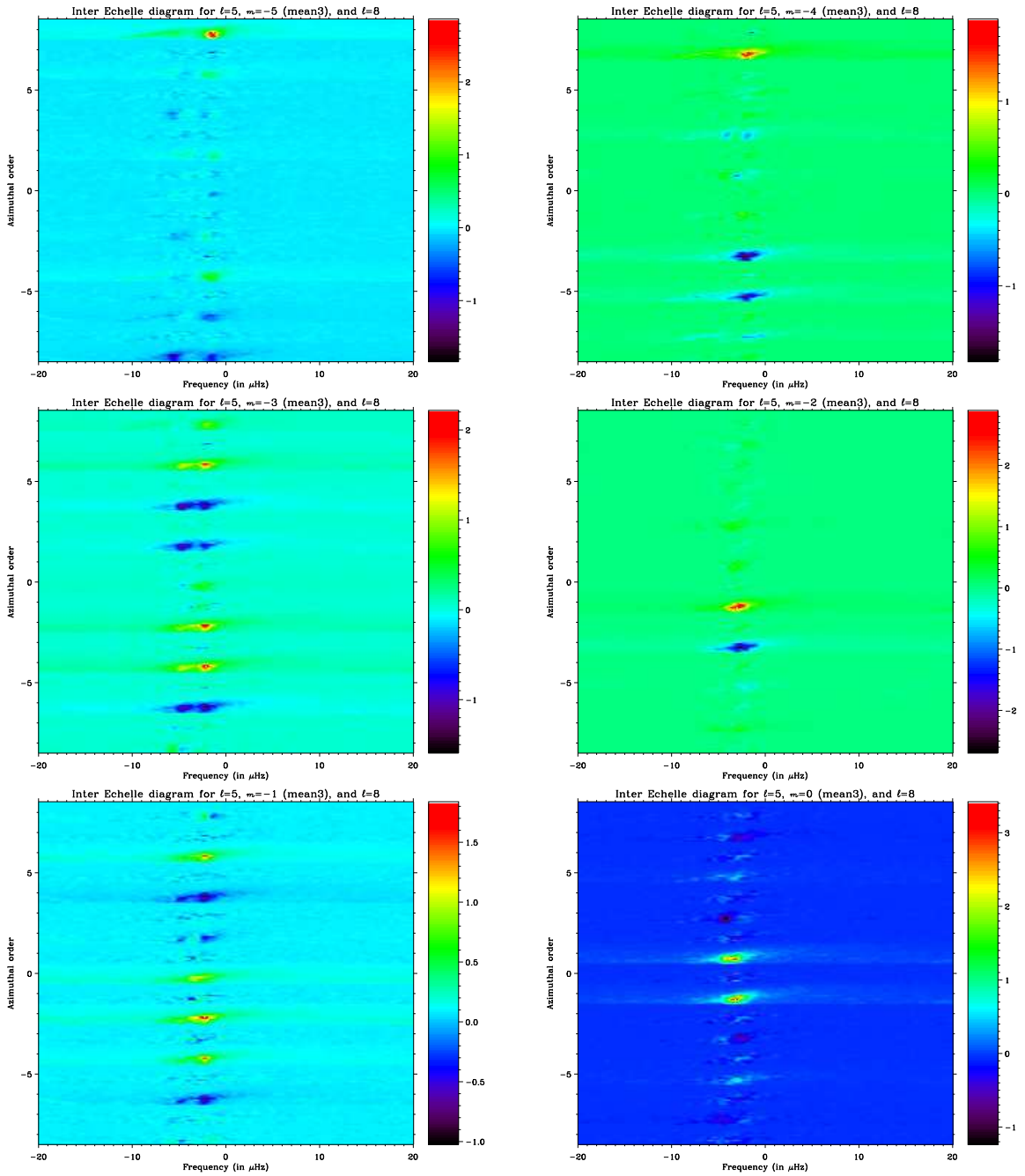

Fig. 13. Inter echelle diagrammes of 1 year of LOI data for $l = 5$ and $l = 8$. (Top, left) For $l = 5, m = -5$. (Top, right) For $l = 5, m = -4$. (Middle, left) For $l = 5, m = -3$. (Middle, right) For $l = 5, m = -2$. (Bottom, left) For $l = 5, m = -1$. (Bottom, right) For $l = 5, m = 0$.

3.2.2. GONG data

The leakage matrices of the GONG data have been computed by R.Howe (1996, private communication). We also computed similar leakage matrices using the equations developed in Part I. The integration was made in the θ, ϕ plane with $\theta_{max} = 65.2°, \phi_{max} = 53.5°$ using the natural apodization function. We also took into account the effect of subtracting the velocity of the Sun seen as a star. It affect the sensitivities of the GONG instrument to the modes observed by integrated sunlight instrument (mainly the modes for which $l + m$ is even). For example the theoretical leakage matrices of $l = 1$ and 2 for GONG are given by:

$$C^{(1,1)} = \begin{pmatrix} 1 & 0 & -0.55 \\ 0 & 1 & 0 \\ -0.55 & 0 & 1 \end{pmatrix}$$

$$C^{(2,2)} = \begin{pmatrix} 1 & 0 & -0.268 & 0 & -0.290 \\ 0 & 1 & 0 & 0.451 & 0 \\ -0.122 & 0 & 1 & 0 & -0.122 \\ 0 & 0.451 & 0 & 1 & 0 \\ -0.290 & 0 & -0.268 & 0 & 1 \end{pmatrix}$$

For $l = 1$, the leakage between $m = -1$ and $m = +1$ is negative due to the subtraction of the mean velocity which affects these modes. For $l = 2$, the leakage between $m = -1$ and $m = +1$ has about the same value as for the LOI; these modes are not affected by the subtraction. The cross echelle diagrammes of the $l = 2$ GONG data are very to those of the LOI (See Fig.10). Figure 14 shows an example of a GONG cross echelle diagramme after having applied the inverse of the leakage matrix.

3.3. Noise covariance matrix measurement

3.3.1. LOI/SOHO data

Figure .15 show the ratio cross spectra of $l = 2$ for the LOI data. As this is commonly the case for the LOI, the ratios are independent of frequency. In addition, as outlined in Part I, the ratio matrix is very close to the leakage matrix. Using Eq. (12) and Fig. 15, one can see that this is the case for the LOI. The ratio matrix has even the same symmetry property as the leakage matrix. In the case of the LOI, we sometimes use the independence of the ratio with frequency to reduce the number of free parameters.

3.3.2. GONG data

Figures 16 and 17 show the ratio cross spectra of $l = 2$ for the GONG data. For the GONG data, the ratio matrices are not symmetrical. Nevertheless, these matrices are still very close to those of the leakage matrices (Eq. (12). It is also clear that the ratios are dependent upon frequency, due probably to the effect of mesogranulation affecting the spatial properties of the noise with frequency. In this case, we cannot reduce the number of parameters to be fitted (See Rabello-Soares and Appourchaux, 1998, in preparation).

4. Summary and conclusion

By visualizing the correlation between the Fourier spectra, one can with:

- the (m, ν) echelle diagramme:
  1. visualizes which degree can be detected,
  2. visualizes the mode splitting,
  3. visualizes spurious degrees,
- the cross echelle diagramme:
  1. verifies the sign of the imaginary parts of the Fourier spectra for $m < 0$
  2. derives the sign of the elements of the leakage matrix of the degree l
  3. verifies to the first order the theoretical leakage matrix of the degree l by applying the inverse of this matrix to the data
- the inter echelle diagramme:
  1. derives the sign of the elements of the full leakage matrix for degrees l, l',
  2. verifies to the first order the theoretical leakage matrix of the degree l, l' by applying the inverse this matrix to the data.
  3. clean the data for aliasing degrees,
- the ratio cross spectrum:
  1. derives the amplitude of the noise correlation between the Fourier spectra
  2. derives the frequency dependence of the correlation

These steps will help to visualize, evaluate the leakage, mode and noise covariance matrices of the observations. The fitting of the p-mode will be considerably eased by verifying that the theoretical knowledge of these matrices is correct.

These steps have been used both on data for which we design the spatial filtering (LOI instrument), and on data for which we did not design the filtering (GONG). As a matter of fact these diagnostics are so powerful that a theoretical knowledge of the various matrices is not always necessary to understand the data. Very often these diagnostics can also be used to find bugs in the data analysis routines (Fig. ??). Nevertheless, it is advisable to know to the first order the leakage and noise covariance matrices for speeding up the analysis process.

Last but not least, the knowledge of the leakage matrices can be used for cleaning the data from unwanted aliasing degrees. This cleaning can be performed either when the pixel time series are available (MDI data, Toutain *et al.* , 1998) or when only the Fourier spectra are available (LOI, GONG). The cleaning has very useful application for the GONG velocity data for removing aliasing degrees from $l = 1, 6$ and 9 for instance, and for inferring better $l = 1$ splittings (Rabello-Soares and Appourchaux 1997). The cleaning is somewhat easier with Fourier spectra as one does need to massage large amount of images.

Acknowledgements. SOHO is a mission of international collaboration between ESA and NASA. Many thanks to Takashi Sekii for constructive comments on the manuscript, and for extensive cyberspace chatting.

References

Appourchaux, T. and Andersen, B.N., 1990, Sol.Phys. 128, 91
Appourchaux, T. and Telljohann, 1996, LOI GSE and VDC specification Doc., Version 1.7, available on the VIRGO home page (ftp://ftp.estec.esa.nl/pub/loitenerife/virgo.html)
Appourchaux, T., Andersen, B.N., Fröhlich, Jiménez, A., Telljohann, U. and Wehrli, C., 1997, Sol. Phys., 170, 27

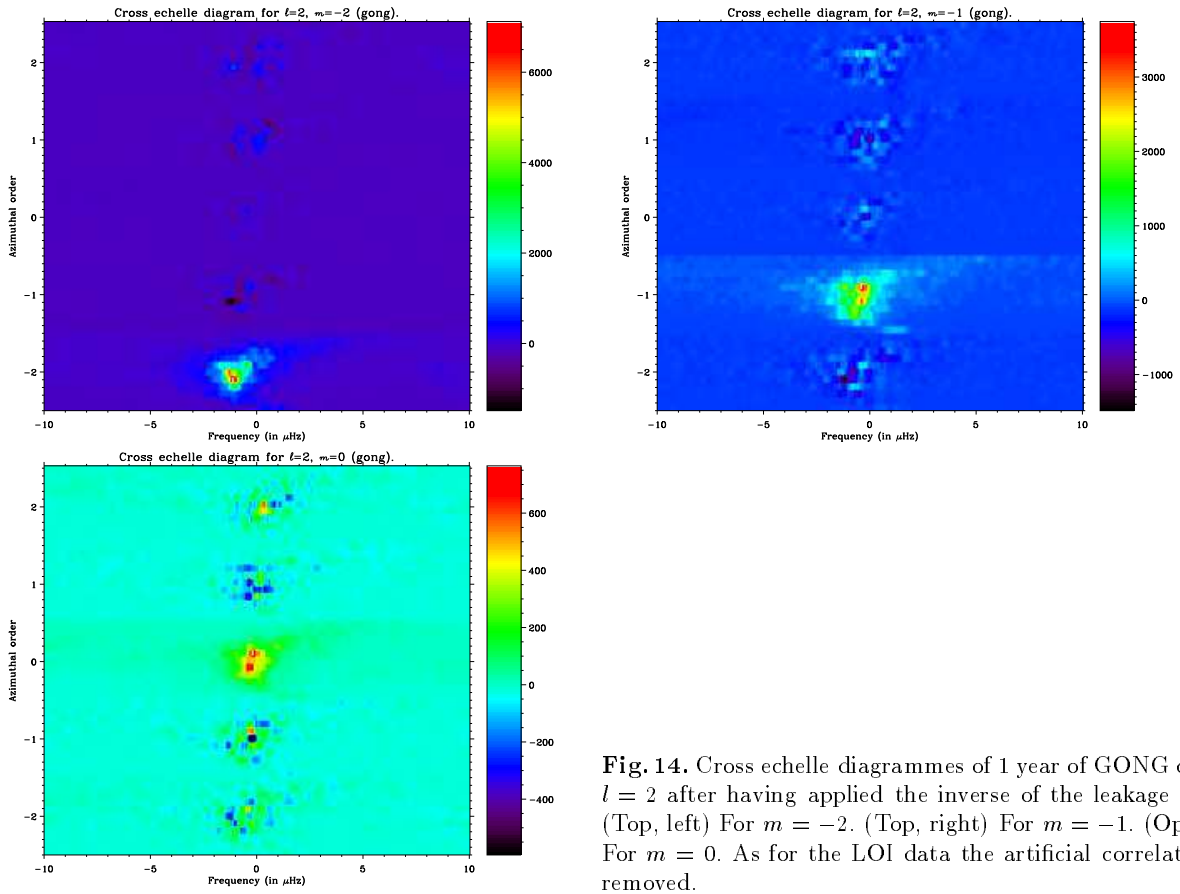

Fig. 14. Cross echelle diagrammes of 1 year of GONG data for $l = 2$ after having applied the inverse of the leakage matrix. (Top, left) For $m = -2$. (Top, right) For $m = -1$. (Opposite) For $m = 0$. As for the LOI data the artificial correlation are removed.

Brown, T., 1985, Nature, 317, 591
Grec, G., PhD thesis, Université de Nice, Nice
Hill, F., Stark, R.T., Stebbins, R.T. *et al.* , 1996, Science, 272, 1292
Schou, J., 1992, PhD thesis, *On the analysis of helioseismic data*, Århus Universitet, Århus
Toutain, T., Kosovichev, A. and Appourchaux, T., 1998, IAU General assembly, Kyoto

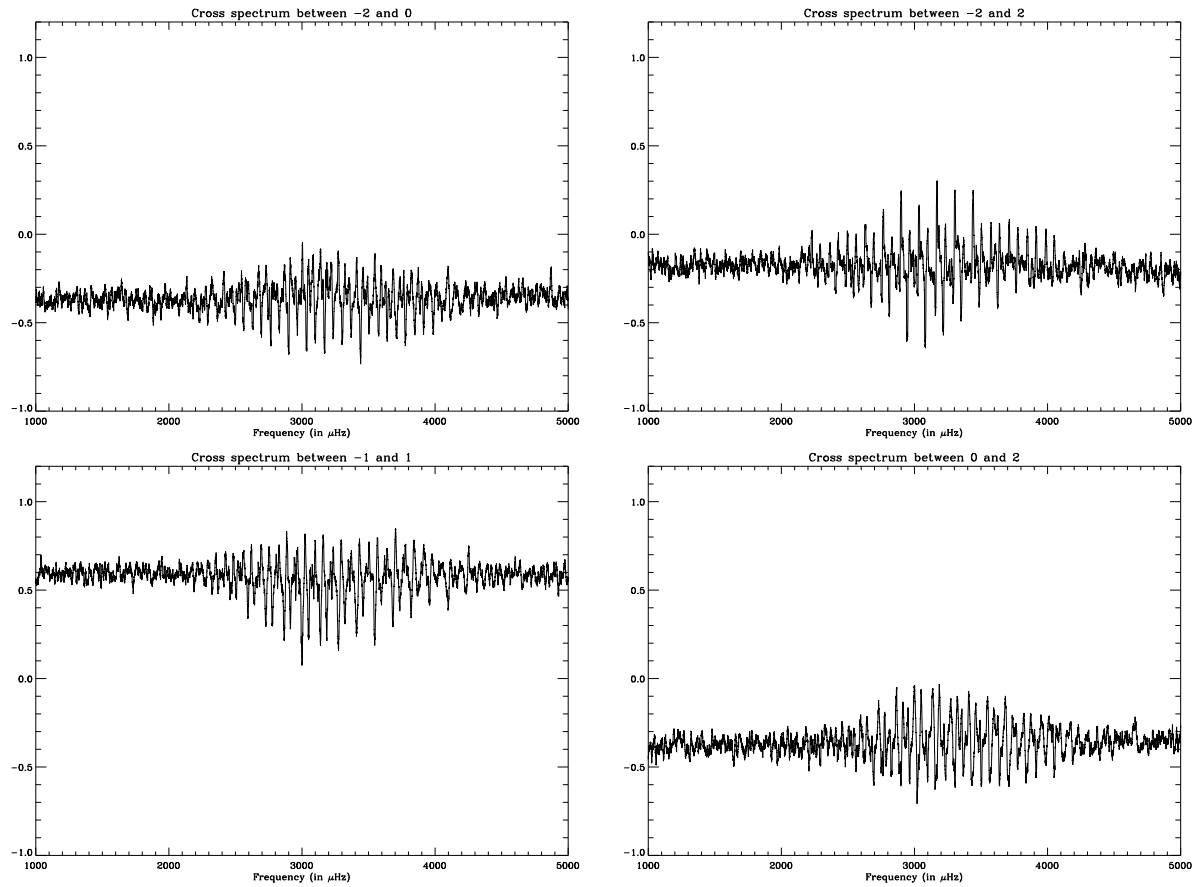

Fig. 15. Ratio cross spectra of $l = 2$ for the LOI data. (Top, left) For $m = -2$ and $m' = 0$. The noise correlation is about -0.45. (Top, right) For $m = -2$ and $m = 2$. The noise correlation is about -0.20. (Bottom, left) For $m = -1$ and $m' = 1$. The noise correlation is about 0.60. (Bottom, right) For $m = 0$ and $m' = 2$. The noise correlation is about -0.35 same as for $m = -2$ and $m' = 0$.

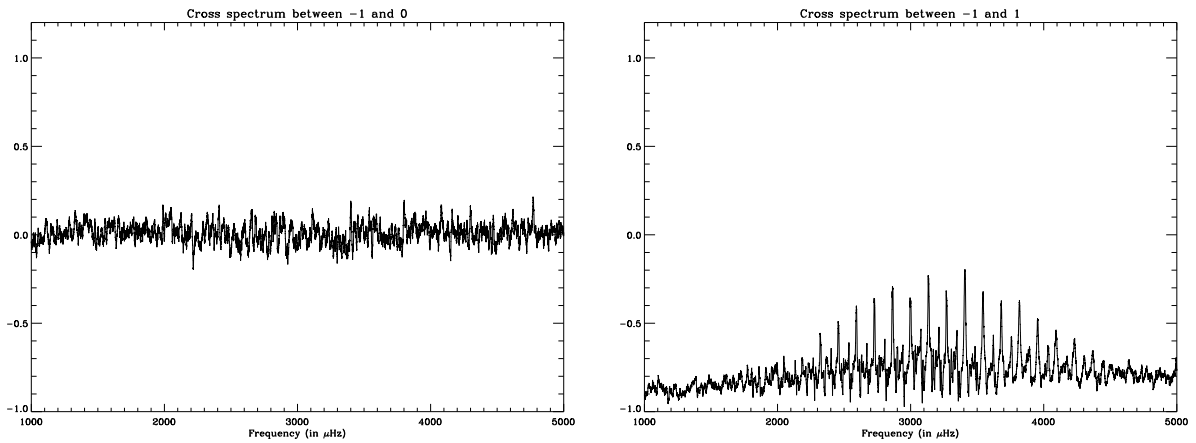

Fig. 16. Ratio cross spectra of $l = 1$ for the GONG data. (Left) For $m = -1$ and m'=0. As for the LOI, there is very little correlation, less than -0.05. The modes also are not seen. (Right) For $m = -1$ and $m = 1$. The noise correlation is -0.77. The correlation is negative because of the way the GONG data are reduced: the full-disk integrated velocity has been removed from the signal.

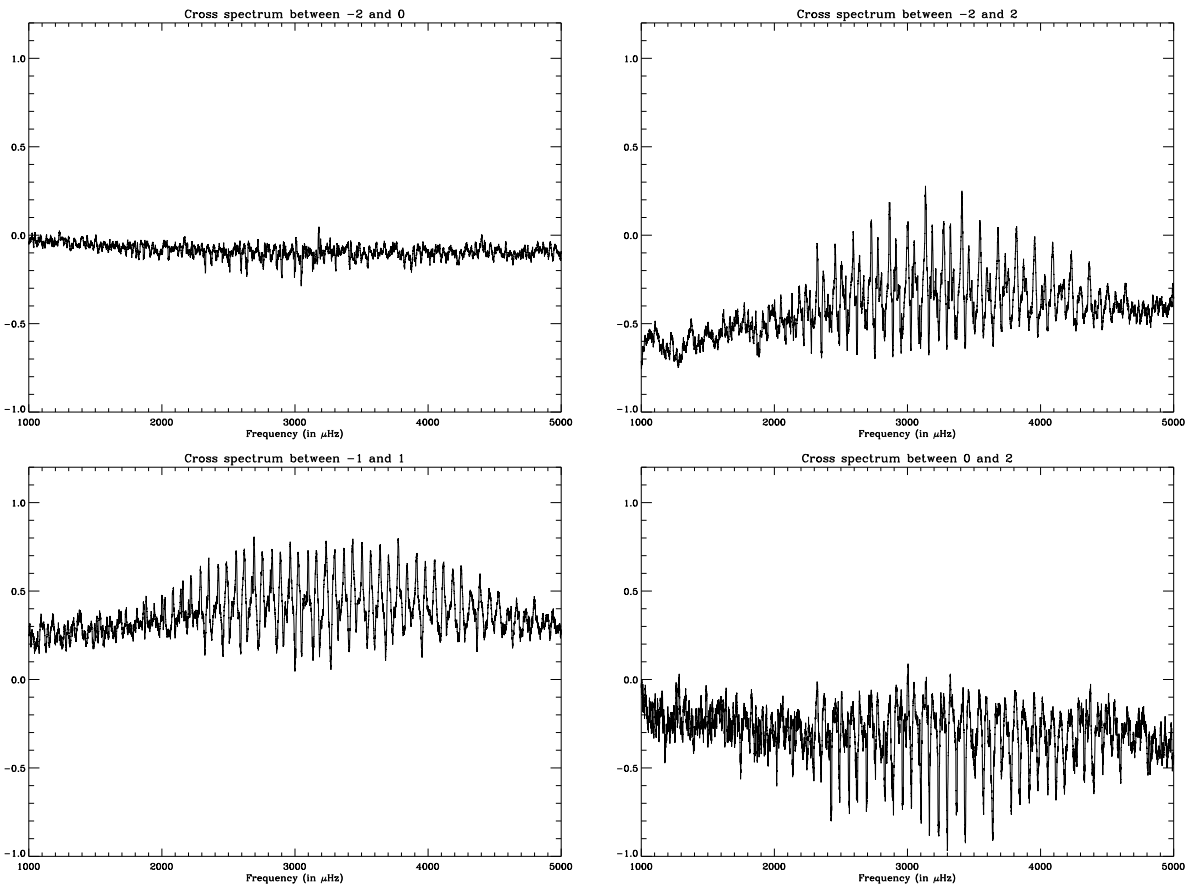

Fig. 17. Ratio cross spectra of $l = 2$ for the GONG data. (Top, left) For $m = -2$ and $m' = 0$. The noise correlation is rather small and about -0.1. (Top, right) For $m = -2$ and $m = 2$. The noise correlation is frequency dependent, with a typical value at 3000 μHz of about -0.3. (Bottom, left) For $m = -1$ and $m' = 1$. The typical value is 0.4. (Bottom, right) For $m = 0$ and $m' = 2$. The typical value is -0.3